

From Realistic NN-Interactions to Cluster Structures in Nuclei: The Interplay of Short and Long-Range Correlations

R. Roth^{*1}, H. Hergert^{*}, T.Neff[†], H. Feldmeier[‡]

^{*} *Institut für Kernphysik, TU Darmstadt, 64289 Darmstadt, Germany*

[†] *NSCL, Michigan State University, 1 Cyclotron, East Lansing, Michigan 48824-1321, USA*

[‡] *Gesellschaft für Schwerionenforschung (GSI), 64291 Darmstadt, Germany*

Abstract

The Unitary Correlation Operator Method (UCOM) provides a novel route towards *ab initio* nuclear structure calculations starting from realistic NN-potentials. The dominant short-range central and tensor correlations are described explicitly by a unitary transformation. The application of UCOM in the context of the no-core shell model provides insight into the interplay between dominant short-range and residual long-range correlations in the nuclear many-body problem. The use of the correlated interaction within Hartree-Fock and Fermionic Molecular Dynamics proves its applicability for nuclear structure calculations across the whole nuclear chart.

Keywords: Nuclear Structure, Realistic NN-Interactions, Unitary Correlation Operator Method, Hartree-Fock, Fermionic Molecular Dynamics

1 Introduction

In recent years several realistic nucleon-nucleon interactions like the Argonne V18 and the CD Bonn potentials have been constructed on the basis of high-precision nucleon-nucleon scattering data. These potentials are used in *ab initio* nuclear structure calculations, e.g., in the framework of the Green's function Monte Carlo method which are presently feasible for nuclei up to mass numbers $A \lesssim 12$ [1]. The use of these realistic potentials for nuclear structure studies in heavier nuclei poses an enormous challenge. Traditional many-body methods, like Hartree-Fock or the multi-configuration shell-model, cannot be used in connection with the bare NN-interaction. The reason is the inability of the restricted model spaces to describe the dominant correlations, which are present in the exact many-body eigenstates.

The two most important types of correlations manifest themselves in the deuteron already. Figure 1 depicts the diagonal elements of the spin-projected two-body density matrix $\rho_{1,M_S}^{(2)}(\mathbf{r})$ for the deuteron calculated with the AV18 potential. Two prominent features of the two-body density distribution are evident: (i) a complete suppression at small relative distances r and (ii) a pronounced angular structure relative to and depending on the spin orientation.

The suppression of the two-body density at small interparticle distances is a direct signature of the *central correlations* induced by the repulsive core in the central part of the realistic potential. For energetic reasons the nucleons avoid the repulsive core which results

¹robert.roth@physik.tu-darmstadt.de

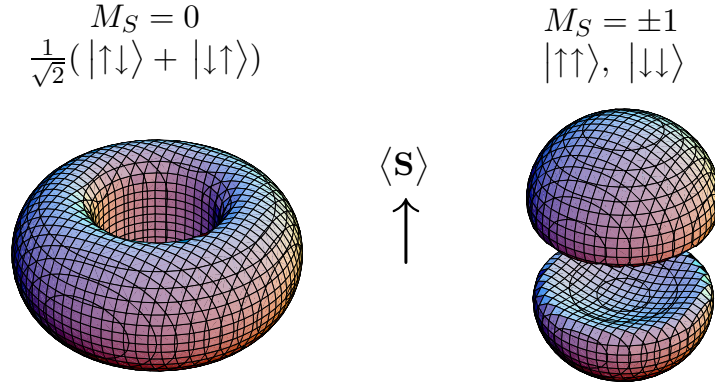


Figure 1: Spin-projected two-body density $\rho_{1,M_S}^{(2)}(\mathbf{r})$ of the deuteron, calculated with the AV18 potential. Shown is an iso-density surface for 0.005 fm^{-3} (taken from [2]).

in a suppression of the probability density for finding two nucleons at small distances. The pronounced angular structure is a manifestation of *tensor correlations*. Depending on the relative alignment of the spins of proton and neutron (parallel for $M_S = \pm 1$ or antiparallel for $M_S = 0$) the spatial two-body density distribution changes dramatically. For $M_S = 0$, the probability density is concentrated in the plane perpendicular to the spin direction (doughnut), whereas the probability density for $M_S = \pm 1$ is largest along the spin axis (dumb-bell). The situation is analogous to the classical dipole-dipole interaction: for parallel dipoles the interaction energy is minimal if the distance vector is parallel to the dipole orientation. For anti-parallel dipoles the distance vectors perpendicular to the dipole moments are energetically favoured. Neither of these correlations can be modelled by a single or a superposition of few Slater determinants. Therefore, a naive inclusion of the bare realistic NN-potential into a Hartree-Fock or multi-configuration shell-model calculation has to fail.

2 Unitary Correlation Operator Method

The basic idea of the Unitary Correlation Operator Method (UCOM) is to include the dominant correlations into the many-body state by means of a unitary transformation [3, 4, 2, 5]. Starting from an uncorrelated many-body state $|\Psi\rangle$, in the simplest case just a Slater determinant, a correlated state $|\tilde{\Psi}\rangle$ is defined through the application of the unitary correlation operator C:

$$|\tilde{\Psi}\rangle = C |\Psi\rangle . \quad (1)$$

Alternatively, one can perform a similarity transformation of the operators of all relevant observables (e.g. the Hamiltonian, coordinate and momentum space densities, transition operators, etc.):

$$\tilde{O} = C^\dagger O C . \quad (2)$$

Due to unitarity both approaches are equivalent. For most many-body calculations the formulation through correlated operators is, however, more convenient.

We decompose the correlation operator C into a central correlator C_r and a tensor correlator C_Ω , reflecting the two dominant types of correlations in the many-body problem:

$$C = C_\Omega C_r = \exp\left[-i \sum_{i<j} g_\Omega(ij)\right] \exp\left[-i \sum_{i<j} g_r(ij)\right]. \quad (3)$$

Both operators are defined as exponentials of Hermitian two-body generators g_Ω and g_r , respectively. They are given in a closed analytic form which reflects the mechanism by which correlations are induced by the interaction.

Central Correlations. The task of the central correlator C_r is to generate the hole in the two-body density distribution at small particle distances caused by the strong repulsive core in the central part of the interaction. Pictorially speaking, C_r has to shift those pairs of particles, which are closer than the core radius, apart from one another. The two-body generator for this distance-dependent shift can be written as $g_r = \frac{1}{2}[s(r)q_r + q_r s(r)]$, where $q_r = \frac{1}{2}[\mathbf{q} \cdot (\mathbf{r}/r) + (\mathbf{r}/r) \cdot \mathbf{q}]$ is the radial component of the relative momentum \mathbf{q} of a particle pair. The function $s(r)$ determines the distance-dependence of the shift. It is large for small r and vanishes for large distances.

Tensor Correlations. The tensor correlation operator C_Ω has to generate the complex angular structure of the two-body density distribution with respect to the spin orientation. Two nucleons with parallel spin are preferentially oriented with their relative position vector aligned with the spin. Nucleons with antiparallel spins prefer relative position vectors perpendicular to the spin direction. The tensor correlator has to generate this angular shift towards or away from the spin direction. An essential ingredient is the component of the relative momentum \mathbf{q} perpendicular to \mathbf{r} , the so-called orbital momentum $\mathbf{q}_\Omega = \mathbf{q} - \frac{\mathbf{r}}{r} q_r$. The generator has the form $g_\Omega = \frac{3}{2}\vartheta(r)[(\boldsymbol{\sigma}_1 \cdot \mathbf{q}_\Omega)(\boldsymbol{\sigma}_2 \cdot \mathbf{r}) + (\mathbf{r} \leftrightarrow \mathbf{q}_\Omega)]$ which is similar to the tensor operator. The function $\vartheta(r)$ describes the magnitude of the shift as a function of distance.

Correlated Operators and Cluster Expansion. For the following many-body calculations, the notion of correlated operators is advantageous. The operators of all observables under consideration have to be transformed consistently. Since the correlation operators are defined as exponentials of two-body operators, the correlated operators contain irreducible contributions for all particle numbers. We organise the different irreducible terms according to their rank in a cluster expansion

$$\tilde{H} = C^\dagger H C = \tilde{H}^{[1]} + \tilde{H}^{[2]} + \tilde{H}^{[3]} + \dots \quad (4)$$

Here we used the Hamiltonian $H = T + V$ as an example, but the same holds true for any other operator. If the range of the correlators is sufficiently small compared to the average

particle distance in the many-body system, three-body and higher order terms in the cluster expansion are small and we can restrict ourselves to the two-body approximation

$$\tilde{H}^{C2} = \tilde{T}^{[1]} + \tilde{T}^{[2]} + \tilde{V}^{[2]} = T + V_{\text{UCOM}}, \quad (5)$$

where $\tilde{T}^{[1]} = T$ and $\tilde{T}^{[2]}$ are the one- and two-body contributions of the correlated kinetic energy, resp., and $\tilde{V}^{[2]}$ is the two-body part of the correlated NN-potential. All two-body contributions are subsumed in the correlated interaction V_{UCOM} . It is by construction *phase-shift equivalent* to the original, uncorrelated NN-potential as long as the correlators have finite range.

Optimal Correlation Functions. The remaining task is the determination of the correlation functions $s(r)$ and $\vartheta(r)$ entering into the generators of the unitary transformations. For each spin-isospin channel they can be obtained from an energy minimisation in the two-body system. This procedure and the optimal correlators for the Argonne V18 (AV18) potential are discussed in Ref. [5]. The tensor correlation functions require a special treatment. Because of its relation to the one-pion exchange, the tensor force is long-ranged, and so are the tensor correlations induced in the two-body system. In a many-body system, the long-range component of the tensor correlations between two nucleons will be screened due to the presence of other nucleons. In anticipation of this effect, we restrict the range of the tensor correlator by a constraint on the integral of the correlation function, $I_\vartheta = \int dr r^2 \vartheta(r)$. Hence, only short-range correlations are described explicitly by the unitary transformation. Long-range correlations have to be covered by the many-body states—this will be illustrated in the following sections.

3 No Core Shell-Model Calculations

As a first application of the correlated realistic interaction V_{UCOM} we consider a straightforward no core shell-model diagonalisation within a harmonic oscillator basis. The shell model itself is able to describe part of the many-body correlations, depending on the size of the model space. Hence the dependence of the energy on the model-space size provides information on the role of short-range correlations and on the contribution from residual long-range correlations. For the calculations we employ the translationally invariant no-core shell model code developed by Petr Navrátil [6], but without using the Lee-Suzuki transformation. The computation of the relevant two-body matrix elements of V_{UCOM} in the harmonic oscillator basis and further results are discussed in Ref. [5].

Figure 2 shows the ground state energy of ${}^4\text{He}$ as a function of the oscillator parameter $\hbar\Omega$ for different sizes of the model space, characterised by the maximum relative oscillator quantum number \mathcal{N}_{max} . The upper panel correspond to a calculation with the bare AV18 potential. Evidently, even for the largest feasible model spaces, the energy does not converge. The reason is that a full description of short-range central and tensor correlations requires even larger model spaces, which are computationally not tractable anymore. The picture changes if we use V_{UCOM} , i.e., include the unitary transformation of the Hamiltonian. The

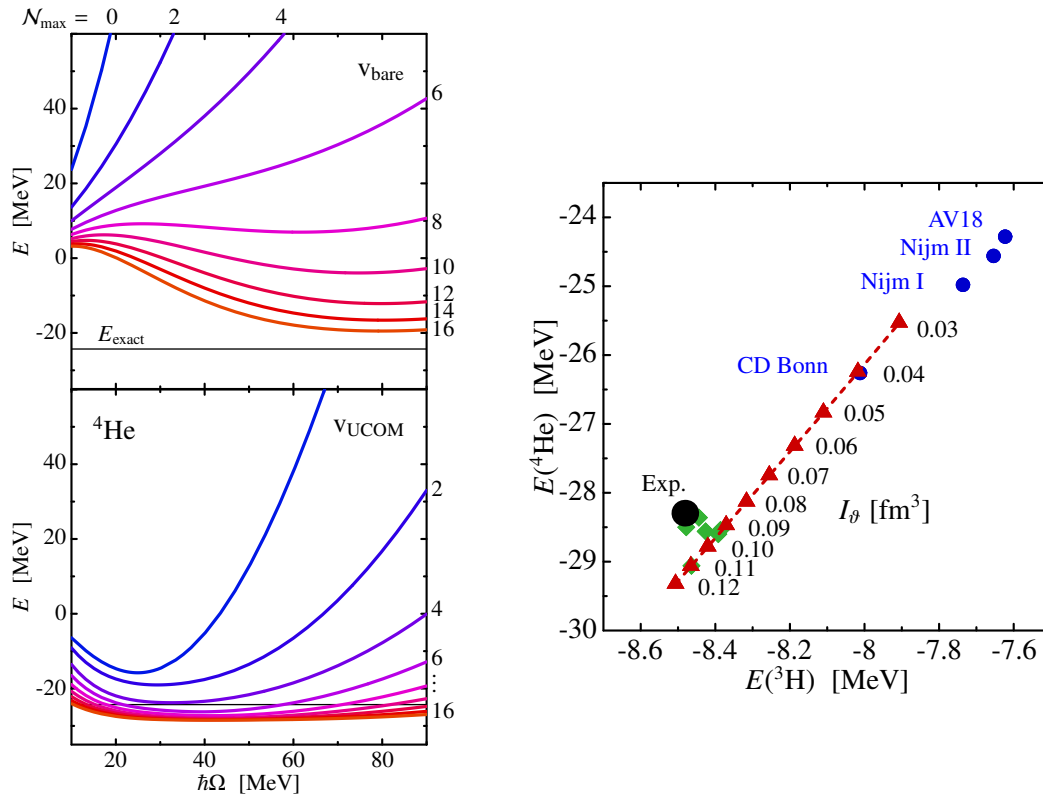


Figure 2: Results of no-core shell model calculations using the correlated AV18 potential. Left panel: convergence of the ground state energy of ^4He for bare (upper plot) and correlated AV18 potential (lower plot). Right panel: Tjon-line and dependence of the energy on the correlator range as described in the text (taken from [5]).

convergence is dramatically improved since now the short-range central and tensor correlations are treated explicitly by the unitary correlation operator. Note, that a bound nucleus is already obtained with a single Slater determinant (i.e. $\mathcal{N}_{\max} = 0$). With increasing size of the model-space, the ground state energy is lowered further. This is the result of the improved description of long-range correlations—not accounted for explicitly by the unitary transformation—by the model space.

A second interesting aspect is illustrated on the right-hand side of Fig. 2, where the converged ground state energies of ^3H and ^4He are plotted. Each data point corresponds to a different interaction. The exact energies for the different bare NN-interactions, like the AV18, the CD Bonn and the Nijmegen interactions (circles), fall onto the so-called Tjon-line [7] but are far away from the experimental point. Three-nucleon interactions (diamonds) are needed to obtain binding energies in the experimental region. The exact energies for the correlated interaction V_{UCOM} based on AV18 (triangles) depend on the range I_ϑ of the triplet-even tensor correlation function. With increasing range the energy is lowered and the full Tjon-line is mapped out. This is related to the omission of three-body (and higher-order)

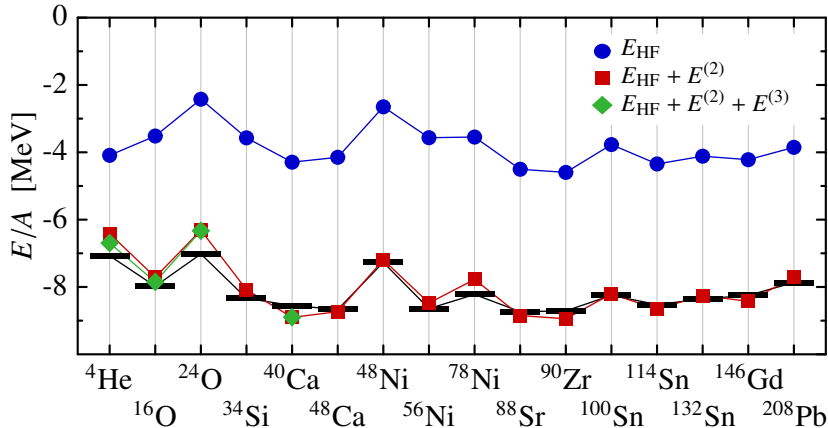


Figure 3: Ground state energy of various closed shell nuclei obtained with the correlated AV18 potential within a HF calculation (circles) and in HF + MBPT (squares and diamonds) in comparison to experimental binding energies (bars) (taken from [8]).

terms in the cluster expansion of the correlated Hamiltonian. If these terms were included, the energies would be exactly the same, independent of the correlator range, because of the unitarity of the transformation. The fact that the range of the tensor correlator can be chosen such that the energies are close to experiment (e.g. for $I_\vartheta = 0.09 \text{ fm}^3$) can be explained by a cancellation between genuine three-body forces and the induced three-body contributions of the cluster expansion. In other words, the impact of the net three-body force on the binding energies can be minimised by a proper choice of the correlator range.

4 Hartree-Fock & Many-Body Perturbation Theory

Using the correlated AV18 interaction we can also perform Hartree-Fock (HF) calculations of nuclear ground states throughout the whole nuclear chart. Since the HF many-body state (Slater determinant) alone is not able to describe any many-body correlations, the use of bare realistic interactions does not lead to bound nuclei. The explicit inclusion of the short-range correlations via the unitary correlation operators is inevitable.

We have implemented the HF scheme in the harmonic-oscillator representation, using the translationally invariant Hamiltonian $H_{\text{int}} = T - T_{\text{cm}} + V_{\text{UCOM}}$, where V_{UCOM} contains charge-dependent and Coulomb terms [8]. The results for ground state energies of closed-shell nuclei ranging from ${}^4\text{He}$ to ${}^{208}\text{Pb}$ are depicted in Fig. 3. The optimal correlator for $I_\vartheta = 0.09 \text{ fm}^3$ is used, and the single-particle basis includes 12 major oscillator shells. Evidently the HF binding energies are significantly smaller than the experimental ones. This is not surprising, since residual long-range correlations as they appeared in the no-core shell model calculations, have not been accounted for.

An estimate for the impact of residual long-range correlations on the binding energies can be obtained within many-body perturbation theory. The evaluation of the second and third order perturbative contribution on top of the HF result is straightforward [8]. Figure 3 sum-

marises the results for the ground state energies including second order correlations (for light nuclei also third order). Again, 12 major oscillator shells are included to obtain a satisfactory degree of convergence for the perturbative correction. The agreement with the experimental binding energies is remarkably good throughout the whole mass range. The absence of any systematic deviation for larger mass numbers proves that the cancellation between genuine three-body force and induced three-body contribution, which we observed in the no-core shell model for light isotopes, works throughout the whole nuclear chart. Furthermore, the calculations establish the perturbative character of the long-range correlations. Note that a perturbative treatment of the short-range correlations is not possible—in our approach they are covered by the unitary correlation operators from the outset.

This opens promising perspectives for the application of other, more refined many-body schemes. The HF solution serves as a starting point for various, more refined methods for the description of nuclear structure and nuclear excitations. We have performed RPA calculations using the same correlated interaction employed here. Large-scale shell-model and Configuration Interaction type calculations are in preparation.

However, the good agreement with experimental data does not hold for all observables. The charge radii obtained in HF for heavier nuclei are too small in comparison to experiment [8]. The inclusion of perturbative corrections improves the result but still leaves a deviation of up to 1 fm for the heaviest nuclei. This is an indication that a net three-body force is needed to reproduce all observables, although its impact on the energy might be small. This issue is the topic of future investigations.

5 Fermionic Molecular Dynamics

In addition to nuclear structure methods working with standard orthonormal single-particle bases, approaches using nonorthogonal Gaussian single-particle states offer a powerful tool for the investigation of strong intrinsic deformations and clustering phenomena. These can be viewed as special types of long-range many-particle correlations, that are very difficult to describe, e.g., in a standard oscillator basis.

To demonstrate this, we perform nuclear structure calculations in the $A \lesssim 60$ region using the Fermionic Molecular Dynamics (FMD) approach [9]. The many-body trial state is given by a simple Slater determinant as in a standard HF scheme

$$|Q\rangle = \mathcal{A}(|q_1\rangle \otimes |q_2\rangle \otimes \cdots \otimes |q_A\rangle) . \quad (6)$$

The coordinate space part of the single-particle states,

$$|q\rangle = \sum_{\nu=1}^n c_{\nu} |a_{\nu}, \mathbf{b}_{\nu}\rangle \otimes |\chi_{\nu}\rangle \otimes |m_t\rangle , \quad (7)$$

however, is given by localised Gaussian wave packets $\langle \mathbf{x} | a_{\nu}, \mathbf{b}_{\nu} \rangle = \exp[-(\mathbf{x} - \mathbf{b}_{\nu})^2 / (2 a_{\nu})]$ with a complex vector \mathbf{b}_{ν} encoding the mean position and mean momentum of the wave packet and a complex width parameter a_{ν} . Several wave packets with different spin orientations $|\chi_{\nu}\rangle$ can be superposed to enhance the flexibility of the single-particle trial states.

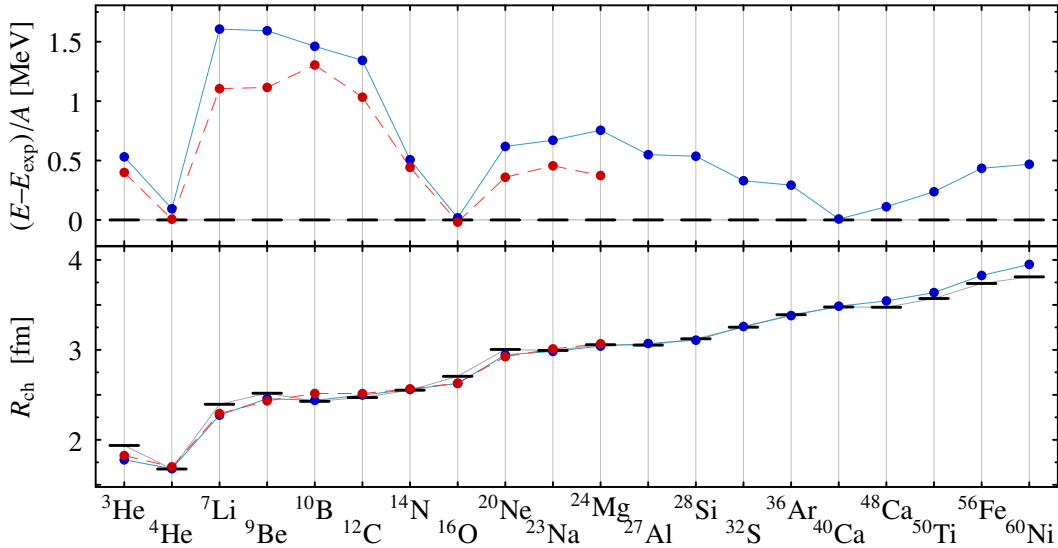


Figure 4: Deviation from the experimental binding energy per nucleon (upper panel) and charge radius (lower panel) for various stable isotopes. Shown are the results with one Gaussian per nucleon (upper circles) and with two Gaussians per nucleon (lower circles) (taken from [2]).

These trial states prove to be extremely versatile: spherical shell-model type states as well as intrinsically deformed and α -cluster configurations can be described.

We perform the large-scale variational calculation (all parameters of all single-particle states are varied independently) using the correlated AV18 interaction. As the standard HF calculations in Sec. 4 show, we cannot expect agreement with experimental data without the inclusion of long-range correlations. Owing to the non-orthogonal character of the single-particle basis, this is not easily possible within FMD. Therefore, as a pragmatic approach, we supplement the correlated interaction by a phenomenological correction adjusted to the binding energies and radii of a few magic nuclei. The details are discussed in [2].

The variational energies and charge radii for nuclei up to $A \sim 60$ are summarised in Fig. 4. Over all, the binding energies and the charge radii show a nice agreement with experimental data. Sizable deviations from the experimental binding energies appear for p -shell and, to a lesser extent, for sd -shell nuclei. This deviation has two origins: (i) A single Gaussian wave packet for the wave function of each nucleon is not optimally suited to describe the exponential tails of the wave functions common for light isotopes. A generalisation of the single particle trial-states by considering a superposition of two Gaussians leads to a significant improvement as illustrated in Fig. 4. (ii) Away from the magic numbers the variational ground states exhibit strong intrinsic deformations.

The intrinsic one-body density distributions for selected nuclei are depicted in Fig. 5. Apart from the spherical symmetric distributions for the doubly magic nuclei, pronounced intrinsic deformations and α -clustering appear. A projection of these intrinsic states onto angular momentum eigenstates becomes necessary and leads to a further reduction of the

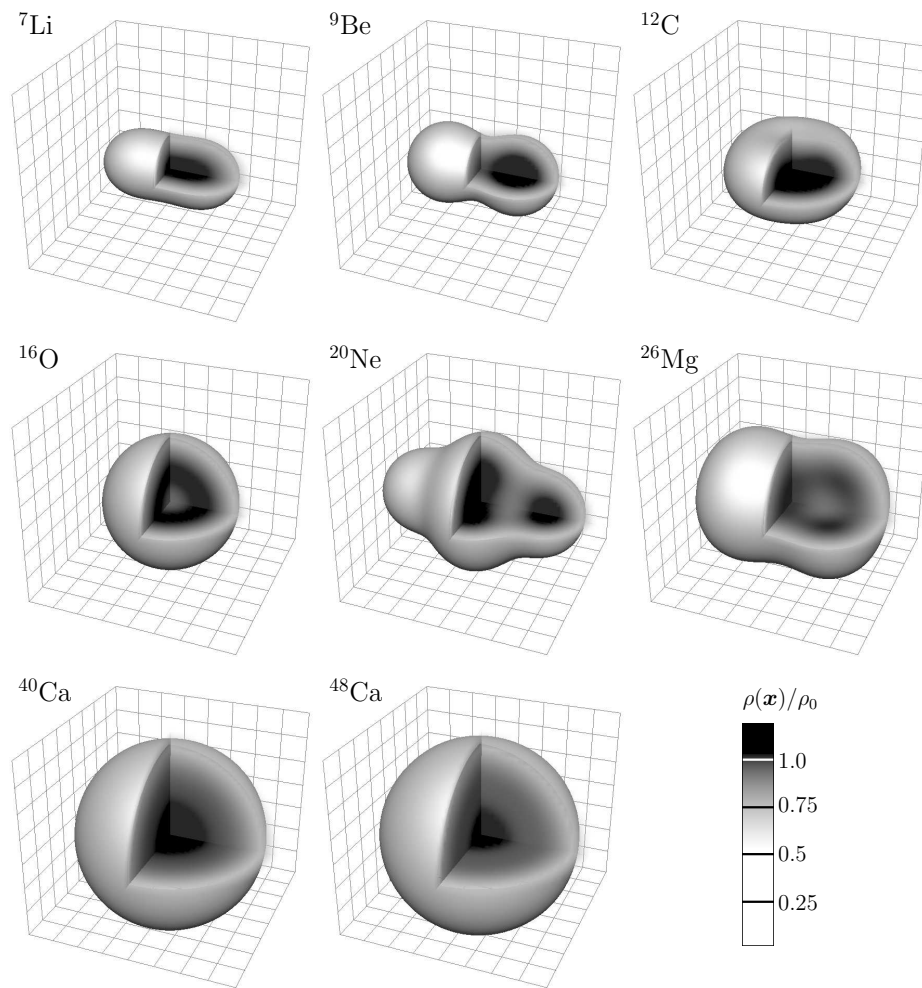


Figure 5: Intrinsic one-body density distributions for various isotopes obtained in variational ground state calculations in the FMD framework (taken from [2]).

ground state energy. At the same time one obtains information on collective rotational states. A detailed discussion of angular momentum projection and multi-configuration calculations within the UCOM/FMD framework is presented in Refs. [2, 10, 11].

6 Conclusions

The Unitary Correlation Operator Method is a promising tool to facilitate nuclear structure calculations on the basis of realistic NN-potentials. The dominant short-range central and tensor correlations are described explicitly by a unitary transformation, which can be used to derive a correlated interaction V_{UCOM} . Residual long-range correlations have to be accounted for by the model space, which due to their perturbative character can be achieved in a variety of many-body approaches. The application of V_{UCOM} in different many-body approaches—ranging from the no-core shell model via Hartree-Fock and perturbation theory to Fermionic Molecular Dynamics—opens new perspectives for a unified understanding of nuclear structure.

Acknowledgements. This work is supported by the DFG through SFB634. We are very grateful to Petr Navrátil for providing us with the no-core shell model code [6].

References

- [1] S. C. Pieper, K. Varga, R. B. Wiringa; *Phys. Rev. C* **66** (2002) 044310.
- [2] R. Roth, T. Neff, H. Hergert, H. Feldmeier; *Nucl. Phys.* **A745** (2004) 3.
- [3] H. Feldmeier, T. Neff, R. Roth, J. Schnack; *Nucl. Phys.* **A632** (1998) 61.
- [4] T. Neff, H. Feldmeier; *Nucl. Phys.* **A713** (2003) 311.
- [5] R. Roth, H. Hergert, P. Papakonstantinou, *et al.*; *Matrix Elements and Few-Body Calculations within the Unitary Correlation Operator Method* (2005); e-Print: nucl-th/0505080; *Phys. Rev. C* (2005) in print.
- [6] P. Navrátil, G. P. Kamuntavicius, B. R. Barrett; *Phys. Rev. C* **61** (2000) 044001.
- [7] A. Nogga, H. Kamada, W. Glöckle; *Phys. Rev. Lett.* **85** (2000) 944.
- [8] R. Roth, P. Papakonstantinou, N. Paar, *et al.*; *Hartree-Fock and Many-Body Perturbation Theory with Correlated Realistic NN-Interactions* (2005); in preparation.
- [9] H. Feldmeier, J. Schnack; *Rev. Mod. Phys.* **72** (2000) 655.
- [10] T. Neff, H. Feldmeier; *Nucl. Phys.* **A738** (2004) 357.
- [11] T. Neff, H. Feldmeier, R. Roth; *Nucl. Phys.* **A752** (2005) 321.